Dyes and Pigments 81 (2009) 167–173

Contents lists available at ScienceDirect

Dyes and Pigments

journal homepage: www.elsevier.com/locate/dyepig

New azo ligands containing azomethine groups in the pyridazine-based chain: Synthesis and characterization

Hamid Khanmohammadi*, Maryam Darvishpour

Department of Chemistry, Arak University, Arak 38156, Iran

ARTICLE INFO

Article history:
Received 12 June 2008
Received in revised form
15 July 2008
Accepted 15 July 2008
Available online 17 October 2008

Keywords:
Azo dye
Schiff base
Pyridazine
Salicylaldehyde derivatives
Solvatochromism
Thermal studies

ABSTRACT

Five, novel pyridazine-based azo chromophores were synthesized by the condensation reaction of 3, 6-bis((aminoethyl)thio)pyridazine with 5-(4-X-phenyl)-azo-salicylaldehyde (X = NO_2, Cl and Et), 5-(2,4-di-Cl-phenyl)-azo-salicylaldehyde and 5-(3,4-di-Cl-phenyl)-azo-salicylaldehyde. The dyes were characterized by elemental analysis, thermal analyses, IR, UV–vis, NMR and mass spectroscopy. Spectral characteristics of the dyes were investigated in four organic solvents of differing polarity; thermal studies indicate that the framework of dyes is stable up to 220 °C. Complexation of the azo dyes with Cu(II) gave subtle changes in their absorption spectra.

1. Introduction

There is at present a considerable interest in synthesis of pyridazine-containing ligands [1–5]. Pyridazine-based ligands are well established as potential bridging units in binuclear complexes since they are capable of spanning two metal ions [6–10]. Usually the 1,2-diazine moiety in pyridazine-based ligands bridges the two metal ions thereby placing them in close proximity to one another. The resulted complexes have a range of interesting properties. For example, the dinuclear metal complexes of pyridazine-containing ligands are capable of mediating strong *anti*-ferromagnetic exchange between the metal ions and tend to stabilise low oxidation states [11–13]. Moreover, the wide spread applications of pyridazine derivatives as dyes and antimicrobial agents have attracted the interest of many investigators [14–17]. These diversified applications are at least in part a consequence of the numerous approaches that are available for the insertion of specific functionalities into the pyridazine nucleus. Prior to this work other groups, most notably Thampson et al. and Brooker et al. reported the synthesis of various cyclic pyridazine-based ligands and their mono- and poly-nuclear metal complexes [18–22]. In contrast, there are relatively few examples of acyclic pyridazine-based Schiff base ligands that also contain phenol groups [23–27].

It has been generally accepted that the strong electronic absorption maximum of azo ligands can be tailored by the presence of various aromatic moieties [28–30]. This, combined with the fact that azo groups are relatively robust and chemically stable, has prompted extensive study of azo-containing Schiff base ligands as dyes and colorants. In order to improve the spectral properties of pyridazine-based ligands, we develop a synthetic route to obtain such ligands containing azo, azomethine, pyridazine and phenol moieties. The choice of these ligands was motivated by two objectives: (i) to provide new acyclic pyridazine-based azo-containing Schiff base ligands and (ii) to study the solvatochromic behavior and thermal stability of new chromophores.

We report here the synthesis and characterization of new family of acyclic azo-containing Schiff base ligands (Scheme 1). The ligands were prepared by condensation reaction of previously prepared diamine (**I**) [21] with azo-coupled salicylaldehyde derivatives, 5-(4-x-phenyl) azo-salicylaldehyde (x = NO_2, Cl and Et), 5-(2,4-di-Cl-phenyl) azo-salicylaldehyde and 5-(3,4-di-Cl-phenyl) azo-salicylaldehyde. The solvatochromic behaviors and substituent effects of the potentially polydentate prepared ligands in various solvents were evaluated. The results indicated that the electronic spectra of the prepared azo ligands were strongly dependent on solvents. The thermal properties of the prepared azo ligands were also examined by thermal gravimetric analysis and indicated that the framework of the prepared azo dyes is stable up to 220 °C.

* Corresponding author. Tel.: +98 861 2777401; fax: +98 861 4173406.
E-mail address: h-khanmohammadi@araku.ac.ir (H. Khanmohammadi).

0143-7208/$ – see front matter © 2008 Elsevier Ltd. All rights reserved.
doi:10.1016/j.dyepig.2008.07.019

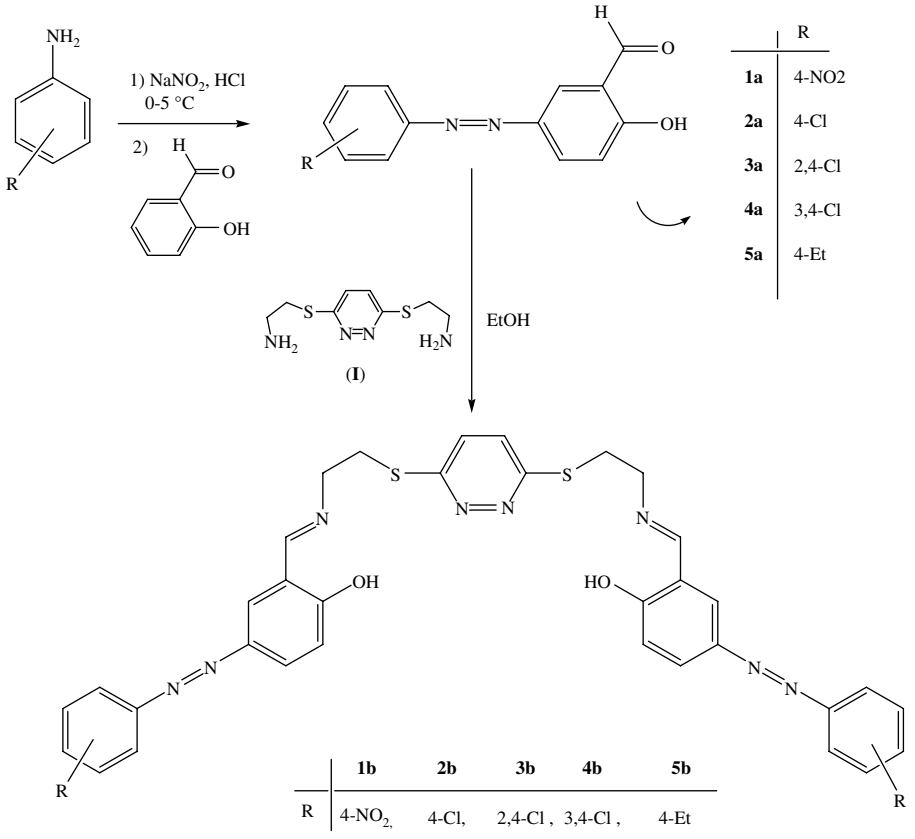

Scheme 1. Azo-linked pyridazine-based ligands.

2. Experimental

2.1. Materials

All of the reagents and solvents involved in synthesis were of analytically grade and used as received without further purification. Salicylaldehyde, *p*-nitroaniline, *p*-chloroaniline, *p*-ethylaniline, 2,4-dichloroaniline and 3,4-dichloroaniline were obtained from Aldrich and Merck. 3,6-Bis((aminoethyl)thio)pyridazine (PTA) (**I**) was prepared as described previously [21].

2.2. Instrumentation

The structure of all synthesized compounds was confirmed by ^{1}H and $^{13}C\{^{1}H\}$ NMR spectra, recorded on a Bruker AV 300 MHz spectrometer. FTIR spectra were recorded as pressed KBr discs, using Unicom Galaxy Series FTIR 5000 spectrophotometer in the region of 400–4000 cm^{-1}. Melting points of all newly prepared compounds were determined on Electrothermal 9200 apparatus. Mass spectra of azo dyes were obtained on Shimadzu QP5050A spectrometer. Thermal analyses were performed on a Perkin–Elmer Thermogravimetric Analyzer TG/DTA 6300 instrument. C, H, N, and S analyses were performed on a Vario EL III elemental analyzer. Electronic spectral measurements were carried out using Perkin–Elmer Lamda double beam spectrophotometer in the range 200–900 nm. Cyclic voltammetry was performed using an Autolab model PGSTAT 20 potentiostat/galvanostat. A glassy carbon disk (1.8 mm diameter) and Pt wire was used as working and counter electrode, respectively.

2.3. Synthesis

2.3.1. General procedure for the synthesis of azo-coupled precursors *1a–5a*

Azo-coupled salicylaldehyde precursors, **1a–5a**, were prepared according to the well-known literature procedure [31,32]. Salicylaldehyde (10 mmol) was dissolved in water (20 ml) containing 10 mmol of sodium hydroxide and 40 mmol of sodium carbonate during the period of 30 min at 0 °C. The resulting solution was added slowly to a solution of diazonium chloride (10 mmol) in water at 0–5 °C. The reaction mixture was stirred for 1 h at 0 °C and then allowed to warm slowly to room temperature. The product was collected by filtration and washed with 100 ml of NaCl solution (10%) under vacuum. The obtained solid was dried under vacuum at 80 °C overnight.

*2.3.1.1. 1-(3-Formyl-4-hydroxyphenylazo)-4-nitrobenzene (**1a**).* Yield: 93.7%, m.p. = 184–186 °C. ^{1}H NMR ($CDCl_3$, ppm): δ 7.18 (d, 1H, $J = 8.96$ Hz), 8.24 (dd, 1H, $J = 8.96$ Hz, $J = 2.35$ Hz), 8.31 (d, 1H, $J = 2.35$ Hz), 8.04 (d, 2H, $J = 8.94$ Hz), 8.42 (d, 2H, $J = 8.94$ Hz), 10.08 (s, 1H), 11.49 (s, 1H). IR (KBr, cm^{-1}); 1657(CHO), 1605(C=C), 1524(N=N), 1478(phenol ring), 1460(NO_2), 1320(NO_2), 1283(C–O), 1103, 852 and 767.

*2.3.1.2. 1-(3-Formyl-4-hydroxyphenylazo)-4-chlorobenzene (**2a**).* Yield: 31.7%, m.p. = 199 °C. ^{1}H NMR (d_6-DMSO, ppm): δ 7.20 (d, 1H, $J = 8.83$ Hz), 8.09 (d, 1H, $J = 8.83$ Hz), 7.64 (d, 2H, $J = 7.23$ Hz), 7.88 (d, 2H, $J = 7.23$ Hz), 8.19 (s, 1H), 10.37 (s, 1H), 11.56 (br, 1H). IR (KBr, cm^{-1}); 1668(CHO), 1618(C=C), 1572(N=N), 1477(phenol ring), 1285(C–O), 1155, 1089, 833 and 725.

*2.3.1.3. 1-(3-Formyl-4-hydroxyphenylazo)-2,4-dichlorobenzene (**3a**).* Yield: 88.13%, m.p. = 120 °C. ^{1}H NMR (d_6-DMSO, ppm): δ 7.29 (d, 1H, J = 8.84 Hz), 8.09 (dd, 1H, J = 8.84 Hz, J = 2.16 Hz), 7.55 (d, 1H, J = 8.76 Hz), 7.68 (d, 1H, J = 8.76 Hz), 7.89 (br, s, 1H), 8.19 (br, s, 1H), 10.37 (s, 1H), 11.88 (br, 1H). IR (KBr, cm^{-1}); 1669(CHO), 1620(C═C), 1577(N═N), 1483(phenol ring), 1285(C–O), 1148, 1055, 837 and 768.

*2.3.1.4. 1-(3-Formyl-4-hydroxyphenylazo)-3,4-dichlorobenzene (**4a**).* Yield: 72.88%, m.p. = 167 °C. ^{1}H NMR (d_6-DMSO, ppm): δ 7.21 (d, 1H, J = 8.87 Hz), 8.10 (dd, 1H, J = 8.87 Hz, J = 2.42 Hz), 7.86 (s, 2H), 8.06 (br, s, 1H), 8.20 (d, 1H, J = 2.42 Hz), 10.37 (s, 1H), 11.69 (br, 1H). IR (KBr, cm^{-1}); 1670(CHO), 1607(C═C), 1572(N═N), 1481(phenol ring), 1285(C–O),1163, 1030, 844 and 764.

*2.3.1.5. 1-(3-Formyl-4-hydroxyphenylazo)-4-ethylbenzene (**5a**).* Yield: 63%, m.p. = 98–100 °C. ^{1}H NMR (d_6-DMSO, ppm): δ 1.22 (t, 3H, J = 6.97 Hz), 2.69 (q, 2H, J = 6.97 Hz), 7.18 (d, 1H, J = 8.82 Hz), 8.08 (d, 1H, J = 8.82 Hz), 7.41 (d, 2H, J = 7.90 Hz), 7.79 (d, 2H, J = 7.90 Hz), 8.16 (s, 1H), 10.37 (s, 1H), 11.54 (br, 1H). IR (KBr, cm^{-1}); 1653(CHO), 1604(C═C), 1578(N═N), 1479(phenol ring), 1277(C–O), 1140, 842 and 758.

*2.3.2. General procedure for the synthesis of dyes **1b–5b***

A solution of 3,6-bis((aminoethyl)thio)pyridazine (PTA) (1 mmol) in absolute EtOH (10 ml) was added to a stirring solution of **1a–5a** (2 mmol) in absolute EtOH during a period of 30 min at 50 °C. The solution was heated in water bath for 2 h at 80 °C with stirring, then cooled and let to stand at ambient temperature. The resulted product was collected by filtration, washed successively with diethyl ether and dried in air.

*2.3.2.1. 3,6-Bis(2-[2-sulfanyl-ethylimino)-methyl]-4-(4-nitro-phenylazo)-phenol pyridazine, C_2H_5OH (**1b**).* Yield: 68.5%, m.p. = 226–230 °C. ^{1}H NMR (d_6-DMSO, ppm): δ 3.63 (t, 4H, J = Hz), 3.95 (t, 4H, J = Hz), 6.78 (d, 2H, J = 9.30 Hz), 7.9 (br, d, 6H), 8.33 (d, 4H, J = 8.63), 7.52 (s, 2H), 8.04 (s, 2H), 8.66 (s, 2H), 13.92 (br, 2H). IR (KBr, cm^{-1}); 1638(C═N), 1612(C═C), 1576(N═N), 1493(phenol ring), 1481(NO_2), 1385, 1362(NO_2), 1275(C–O), 1152, 1086 and 837. $[M]^+$ = 737 molecular ion peak; 692 $[M]^+-NO_2$; 78 [M] peak of Ph–H; 63 [M−1] peak of S_2. Anal. Calcd. for $C_{36}H_{34}N_{10}O_7S_2$: C, 55.23; N, 17.89; H, 4.38; S, 8.19. Found: C, 55.6; N, 18.1; H, 4.6; S, 8.4%.

*2.3.2.2. 3,6-Bis(2-[2-sulfanyl-ethylimino)-methyl]-4-(4-chloro-phenylazo)-phenol pyridazine (**2b**).* Yield: 49%, m.p. = 227–230 °C. ^{1}H NMR (d_6-DMSO, ppm): δ 3.63 (t, 4H, J = 5.77 Hz), 3.95 (t, 4H, J = 5.77 Hz), 6.89 (br, d, 2H, J = 9.05 Hz), 7.89 (dd, 2H, J = 9.05 Hz, J = 2.17 Hz), 7.58 (d, 4H, J = 8.55 Hz), 7.79 (d, 4H, J = 8.55 Hz), 7.51 (s, 2H), 8.01 (s, 2H), 8.69 (s, 2H), 14.00 (br, 2H). IR (KBr, cm^{-1}); 1643(C═N), 1614(C═C), 1588(N═N), 1510(phenol ring), 1389, 1285(C–O), 1145, 1103 and 856. $[M]^+$ = 714 molecular ion peak; 139 $[M]^+-$ pyridazine(S–CH_2CH_2–NCH–Ph(OH))$_2$; 78 [M] peak of Ph–H; 63 [M−1] peak of S_2. Anal. Calcd. for $C_{34}H_{28}Cl_2N_8O_2S_2$: C, 57.06; N, 15.66; H, 3.94; S, 8.96. Found: C, 56.7; N, 14.9; H, 4.3; S, 8.6%.

*2.3.2.3. 3,6-Bis(2-[2-sulfanyl-ethylimino)-methyl]-4-(2,4-dichloro-phenylazo)-phenol pyridazine C_2H_5OH (**3b**).* Yield: 68.7%, m.p. = 105 °C. ^{1}H NMR (d_6-DMSO, ppm): δ 3.62 (t, 4H, J = 5.76 Hz), 3.94 (t, 4H, J = 5.76 Hz), 6.82 (br, d, 2H, J = 9.23 Hz), 7.88 (dd, 2H, J = 9.23 Hz, J = 2.38 Hz), 8.00(d, 2H, J = 2.38 Hz), 7.61 (d, 2H, J = 8.72 Hz), 7.49 (dd, 2H, J = 8.72 Hz, J = 1.98 Hz), 7.80 (d, 2H, J = 1.98 Hz), 7.53 (s, 2H), 8.67 (s, 2H), 14.03 (br, 2H). IR (KBr, cm^{-1}); 1638(C═N), 1614(C═C), 1577(N═N), 1402, 1373, 1285(C–O), 1147, 1099 and 835. $[M]^+$ = 784 molecular ion peak is not observed, but [M−2] = 782 (Cl-35 isotopes); 145 $[M]^+-$Pyridazine (S–CH_2CH_2–NCH–Ph(OH)–N_2)$_2$; 78 [M] peak of Ph–H; 63 [M−1] peak of S_2. Anal. Calcd. for $C_{36}H_{32}Cl_4N_8O_3S_2$: C, 52.05; N, 13.49; H, 3.88; S, 7.72. Found: C, 51.6; N, 13.9; H, 3.5; S, 8.2%.

*2.3.2.4. 3,6-Bis(2-[2-sulfanyl-ethylimino)-methyl]-4-(3,4-dichloro-phenylazo)-phenol pyridazine H_2O (**4b**).* Yield: 71.42%, m.p. = 218–220 °C. ^{1}H NMR (d_6-DMSO, ppm): δ 3.63 (t, 4H, J = 5.94 Hz), 3.94 (t, 4H, J = 5.94 Hz), 6.83 (d, 2H, J = 9.20 Hz), 7.52 (s, 2H), 7.76–8.06 (m, 10H), 8.64 (s, 2H), 14.03 (br, 2H). IR (KBr, cm^{-1}); 1636(C═N), 1606(C═C), 1579(N═N), 1491(phenol ring), 1386, 1288(C–O), 1146 and 826. $[M]^+$ = 784 molecular ion peak; 145 $[M]^+-$ Pyridazine(S–CH_2CH_2–NCH–Ph(OH)–N_2)$_2$; 78 [M] peak of Ph–H; 63 [M−1] peak of S_2. Anal. Calcd. for $C_{34}H_{28}Cl_4N_8O_3S_2$: C, 50.88; N, 13.96; H, 3.52; S, 7.98. Found: C, 51.0; N, 13.6; H, 3.8; S, 7.8%.

*2.3.2.5. 3,6-Bis(2-[2-sulfanyl-ethylimino)-methyl]-4-(4-ethyl-phenylazo)-phenol pyridazine (**5b**).* Yield; 72.7%, m.p. = 185–186 °C. ^{1}H NMR (d_6-DMSO, ppm): δ 1.21 (t, 6H, J = 7.41 Hz), 2.67 (q, 4H, J = 7.41 Hz), 3.63 (t, 4H, J = 5.56 Hz), 3.95 (t, 4H, J = 5.56 Hz), 6.92 (d, 2H, J = 9.00 Hz), 7.89 (d, 2H, J = 9.00 Hz), 7.37 (d, 4H, J = 8.00), 7.73 (d, 4H, J = 8.00), 7.52 (s, 2H), 8.00 (s, 2H), 8.70 (s, 2H), 14.05 (br, 2H). IR (KBr, cm^{-1}); 1636(C═N), 1604(C═C), 1575(N═N), 1489(phenol ring), 1389, 1283(C–O), 1148 and 845. $[M]^+$ = 702 molecular ion peak is not observed, but 436 $[M]^+$–N_2–Ph–CH_2CH_3; 252 $[M]^+-$ Pyridazine(S–CH_2CH_2–)$_2$; 105 [M] peak of Ph–CH_2CH_3; 78 [M] peak of Ph–H; 63 [M−1] peak of S_2. Anal. Calcd. for $C_{38}H_{38}N_8O_2S_2$: C, 64.93; N, 15.94; H, 5.45; S, 9.12. Found: C, 64.6; N, 15.8; H, 5.3; S, 9.4%.

3. Result and discussion

The condensation reaction of 3,6-bis((aminoethyl)thio)pyridazine (PTA) with azo-coupled salicylaldehyde precursors (**1a–5a**) in ethanol, gave good yield of new dyes containing azo, azomethine, pyridazine and phenol moieties (**1b–5b**). All prepared compounds are air stable solids, intensely colored (in the solid state they appear deep red to brown in color), soluble in DMF, THF and DMSO and had elemental analyses consistent with the formulations given in Section 2.

3.1. IR spectra of the compounds

In order to clarify the mode of bonding, the IR spectra of azo-coupled salicylaldehyde precursors (**1a–5a**) and pyridazine-based azo dyes (**1b–5b**) were studied and assigned based on a careful comparison of the latter with the former. A strong band observed in the spectra of **1a–5a** in the region of 1657–1670 cm^{-1} can be assigned to the υ(C═O) group [31]. The total absence of υ(C═O) absorption in the IR spectra of **1b–5b** together with the appearance of new υ(C═N) absorption in the range of 1636–1643 cm^{-1} clearly indicated that a new Schiff base ligand had formed in each case. The IR spectra of **1a–5a** and **1b–5b** show strong band at 1275–1290 cm^{-1} assigned to the C–O stretching mode.

3.2. ^{1}H NMR spectra

^{1}H NMR and ^{13}C{^{1}H} NMR results, obtained for all prepared compounds at ambient temperature in d_6-DMSO and/or $CDCl_3$, are presented in Section 2. The slightly broad signal at δ_H 13.90–14.05 ppm in the ^{1}H NMR spectra of **1b–5b** is assigned to the OH protons, as was confirmed by deuterium exchange when D_2O was added to d_6-DMSO solution. The CH═N protons of **1b–5b** exhibit a singlet resonance at δ_H 8.64–8.70 ppm. The ^{1}H NMR spectra of **1b–5b,** show a singlet resonance in the region δ_H 7.51–7.53 ppm assigned to the pyridazine ring protons.

3.3. The electronic absorption spectra of **1b–5b** in organic solvents of different polarity

The electronic spectra of the pyridazine-based azo dyes were measured in four organic solvents, DMSO, DMF, THF and CH_2Cl_2, at room temperature. The wavelengths of maximum absorbance and molar extinction coefficients are reported in Table 1.

The UV–vis absorption spectra of the azo-coupled salicylaldehyde precursors (**1a–5a**) display mainly two bands arising from the $\pi \rightarrow \pi^*$ transitions in the backbone. The first band located at 264–275 nm can be assigned to the moderate energy transition of the aromatic ring while the second band at 310–345 nm is due to low energy transition [33].

The UV–vis absorption spectra of **1b–5b** in DMSO and DMF display mainly three bands and give a red shift with respect to the same spectra of azo-coupled precursors. The broad band observed in the range 430–485 nm can be assigned to an $n \rightarrow \pi^*$ electronic transition of azo-aromatic chromophore [33,34] and intramolecular charge transfer interaction involving the whole molecules of the prepared dyes. The broadness of the intramolecular CT band is quite common for azo or azomethine dyes having a hydroxyl group in *o*-position to the N=N or C=N bond on the aromatic ring [33].

3.3.1. Solvent effects on absorption spectra of **1b–5b**

It has been accepted that the electronic transitions of azo-azomethine ligands strongly depend on the nature of media [33,35]. For this purpose, the electronic absorption spectra of the prepared dyes, **1b–5b,** were measured in four organic solvents of different polarity namely DMF, DMSO, THF and CH_2Cl_2 at a concentration approximately 10^{-5} M. The absorption curves of **1b** in various solvents are shown in Fig. 1 (see Supplementary material).

We found that the absorption band at 340–404 nm generally shows bathochromic shift (positive solvatochromism) as the polarity of solvent was increased. The influence of solvents for the prepared dyes increases in the order DMSO > DMF > THF > CH_2Cl_2. This observed behavior is accounted as that the prepared azo dyes in the ground state and in the excitation state indicate different polarities. The other band at 430–485 nm shows hypsochromic shift (negative solvatochromism) upon increasing solvent polarity (Table 1), indicating a reduction in the dipole moment upon electronic excitation. The observed hypsochromic displacement of the lowest energy absorption from CH_2Cl_2 to DMSO, being more pronounced for **3b**.

Table 1
Absorption spectral data of **1b–5b** in various organic solvents; λ_{max}/nm (ε/dm mol^{-1} cm^{-1}).

Compounds	DMSO	DMF	THF	CH_2Cl_2
1b	269 (46000) 404 (36600) 480 (31600)	271 (49600) 387 (40000) 476 (22600)	267 (13000) 382 (15000) 477 (3400)	233 (34000) 273 (34600) 378 (40200) 483 (7400)
2b	270 (65000) 366 (65400) 435 (31800)	274 (67200) 365 (70800) 436 (28000)	248 (62000) 287 (44600) 352 (64000) 442 (9400)	250 (65000) 271 (69200) 352 (67600) 446 (9000)
3b	268 (55600) 373 (51400) 436(23000)	270 (53600) 270 (53600) 440 (24600)	249 (50200) 289 (43400) 370 (62000) 455 (12000)	247 (54000) 270 (56400) 366 (62000) 459 (7400)
4b	266 (52000) 379 (51400) 435 (35600)	270 (54200) 370 (55400) 438 (24600)	248 (64200) 289 (52800) 364 (70400) 448 (14400)	243 (53600) 271 (52400) 359 (57800) 451 (7800)
5b	270 (58400) 363 (53600) 435 (21000)	269 (44600) 342 (52200) 435 (9600)	240(36600) 261 (27000) 339 (53000) 442 (2800)	234 (47800) 266 (32600) 338 (53600) 446 (3400)

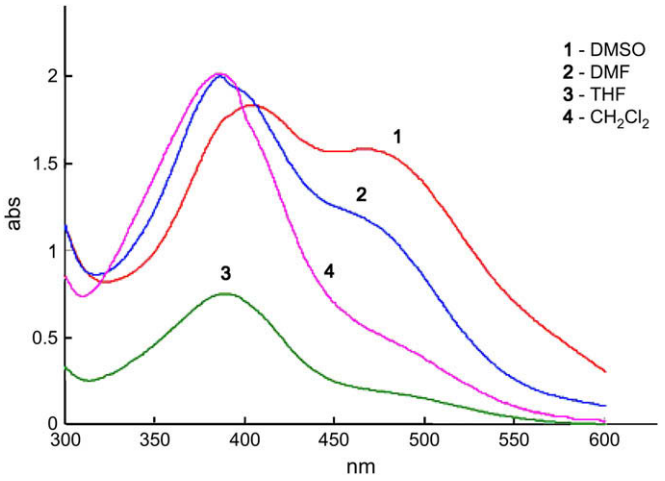

Fig. 1. Absorption spectra of **1b** in various organic solvents.

3.3.2. Substituent effects on absorption spectra of pyridazine-based azo dyes in various solvents

Absorption spectra of the new prepared dyes, with various electron donating or accepting abilities, in DMSO, are shown in Fig. 2. It can be found that the 340–404 and 430–485 nm bands are substantially in the order, **1b** > **3b** > **4b** > **2b** ≥ **5b**. When introducing the nitro group in the aryl azo component of the dye, **1b**, instead of chloride or ethyl groups, the absorption spectra give a remarkable blue shift in all organic solvents compared to the corresponding spectrum of **2b** and **5b**. This means that **1b** has a more extended conjugation than others.

3.4. Electrochemistry of pyridazine-based azo dyes

On scanning from 1.5 V to −1.5 V, the cyclic voltammogram for **5b** (0.5 mmol l^{-1} in a solution containing 80% DMSO and 20% aqueous $LiClO_4$) exhibits three reversible reduction waves (Fig. 3). The first wave is observed at −0.5 V. This reduction process may be due to the partial reduction of the imine bonds to secondary amines (and subsequent protonation by phenol) [23]. This process may also

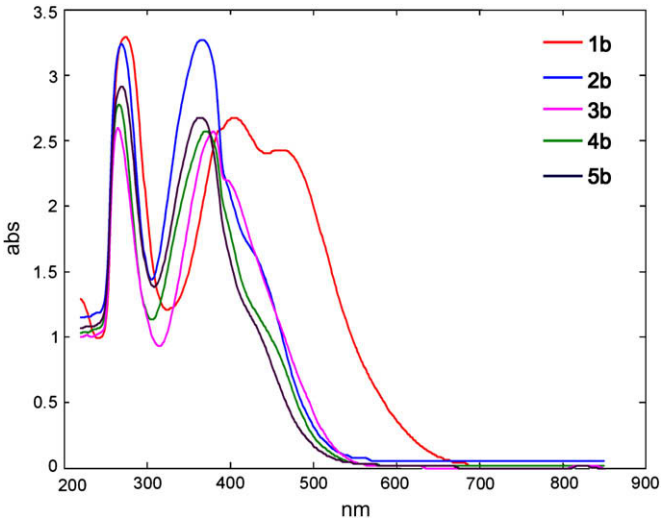

Fig. 2. Effects of substituents on absorption spectra of the prepared compounds **1b–5b** in DMSO.

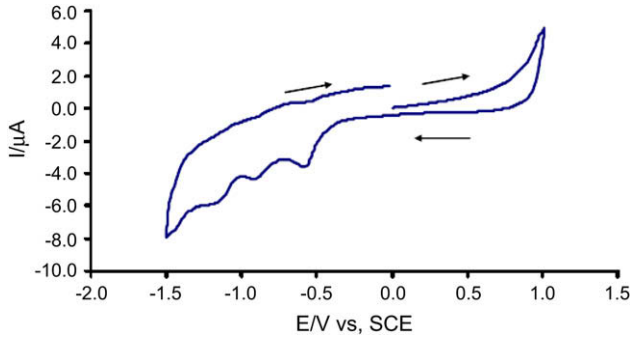

Fig. 3. Cyclic voltammogram for 5×10^{-5} M of **5b** in a solution containing 80% DMSO and 20% aqueous $LiClO_4$.

be associated with the reduction of the azo bonds, however, it should be noted that the possibility that some or all of these processes may instead be based on the pyridazine ring cannot be ruled out [36]. The second and third waves were observed at −0.8 V and −1.1 V, respectively.

Unfortunately, the other azo dyes (**1b**–**4b**) were too insoluble in DMSO for standard electrochemistry study.

3.5. Changes in absorption spectra of *1b–5b* under complexation with copper(II) ion

The effect of addition of copper(II) ions to DMSO solution of the prepared pyridazine-based azo dyes were studied. At each addition

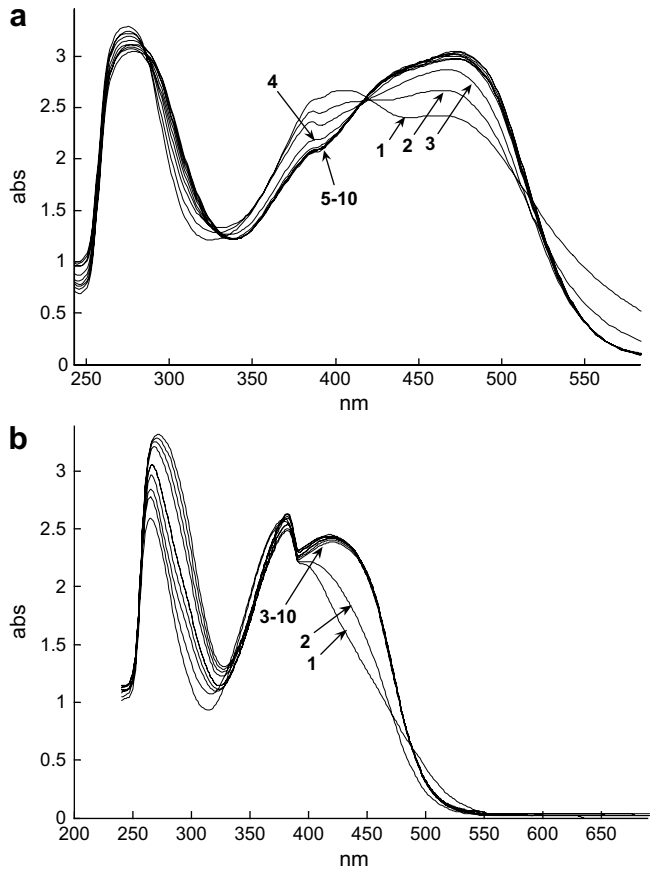

Fig. 4. Changes observed in UV–vis absorption spectra of **1b**, (a) and **4b**, (b) in DMSO, on progressive addition of Cu(II) ion. Numbers indicate a change in absorption with increases in the concentration of Cu(II) (mol l^{-1}); from down to up 0, 1.32×10^{-5}, 2.64×10^{-5}, 3.96×10^{-5}, 5.28×10^{-5}, 6.6×10^{-5}, 7.92×10^{-5}, 10.52×10^{-5}, 11.88×10^{-5}, 13.2×10^{-5}.

Table 2
Thermal analyses data for **1b**–**5b**.

Compound, M.F. (M. Wt.)	Dissociation stages	Temperature range in TG (°C)	Weight loss, found (calculated) (%)	Decomposition assignment
1b, $C_{36}H_{34}N_{10}O_7S_2$ (782.8)	Stage I	80–230	5.46 (5.87)	The loss of 1 C_2H_5OH
	Stage II	240–290	22.70 (22.80)	The loss of $2NO_2 + C_6H_4$
	Stage III	300–530	17.98 (18.01)	The loss of $C_6H_5N_2$
2b, $C_{34}H_{28}Cl_2N_8O_2S_2$ (715.7)	Stage I	245–285	26.10 (26.58)	The loss of $C_5H_6N_2O_2S_2$
	Stage II	300–530	18.89 (19.62)	The loss of C_7H_5N
3b, $C_{36}H_{32}N_8O_3Cl_4S_2$ (830.6)	Stage I	110–130	5.61(5.53)	The loss of 1 mol C_2H_5OH
	Stage II	225–290	28.15(27.70)	The loss of $C_5H_5N_4O_2S_2$
	Stage III	300–530	21.20(21.03)	The loss of $C_7H_7N_2$
4b, $C_{34}H_{28}N_8O_3Cl_4S_2$ (802.6)	Stage I	100–230	1.95(2.20)	The loss of 1 mol H_2O
	Stage II	240–290	27.61(27.81)	The loss of $C_5H_6N_4O_2S_2$
	Stage III	300–530	21.65 (21.03)	The loss of $C_7H_7N_2$
5b, $C_{38}H_{38}N_8O_2S_2$ (702.9)	Stage I	235–275	25.72(25.10)	The loss of $C_4H_4N_2O_2S_2$
	Stage II	280–530	20.40(20.30)	The loss of C_8H_9N

10 μl of $Cu(ClO_4)_2$ solution, prepared in DMSO at the concentration of 3.3×10^{-3} M, was poured into the 2.5 ml DMSO solution of *ca.* 7×10^{-5} M azo dye. After each addition, changes in absorbances of compound were monitored. The absorption peak of dyes at 430–485 nm undergoes a red shift in position till 50 μl of Cu(II) solution is added, after which no further change occurs. The red shift from 430–485 nm to 445–493 nm indicated that Cu(II) ion is mainly complexed with the non-bonding electron pair of the oxygen atom belonging to the hydroxyl group. Also, small red shift in the position of absorption peak at 340–404 nm ($\pi \rightarrow \pi^*$ transitions) is due to the complexation of copper(II) ion with imine or azo groups (Fig. 4).

3.6. Thermal properties

In order to give more insight into the structure of **1b**–**5b**, the thermal studies of the compounds have been carried out using thermogravimetry (DTA–TG) techniques. The thermogravimetric studies have been made in the temperature range 50–550 °C in air. The TG–DTA results (Table 2) indicate that the framework of the prepared azo dyes is stable up to 220 °C (see Supplementary material). Above 230 °C, the TG curves of the prepared compounds show a major loss of weight where the corresponding DTA curves show an exothermic peak. The exothermic peak indicates decomposition of the azo dyes backbone. The comparison of T_d (decomposition temperature) showed that the thermal stability of the azo dyes increases in the order **5b** > **3b** > **2b** > **1b** > **4b** (Table 3). Above 300 °C, the TG curves of **1b**–**5b** show continuous significant weight loss up to 550 °C.

Table 3
Decomposition temperature of **1b**–**5b**.

Compounds	T_d[a]	Compounds	T_d[a]
1b	258.62	**4b**	257.67
2b	263.31	**5b**	265.96
3b	265.08		

[a] Data obtained from TGA.

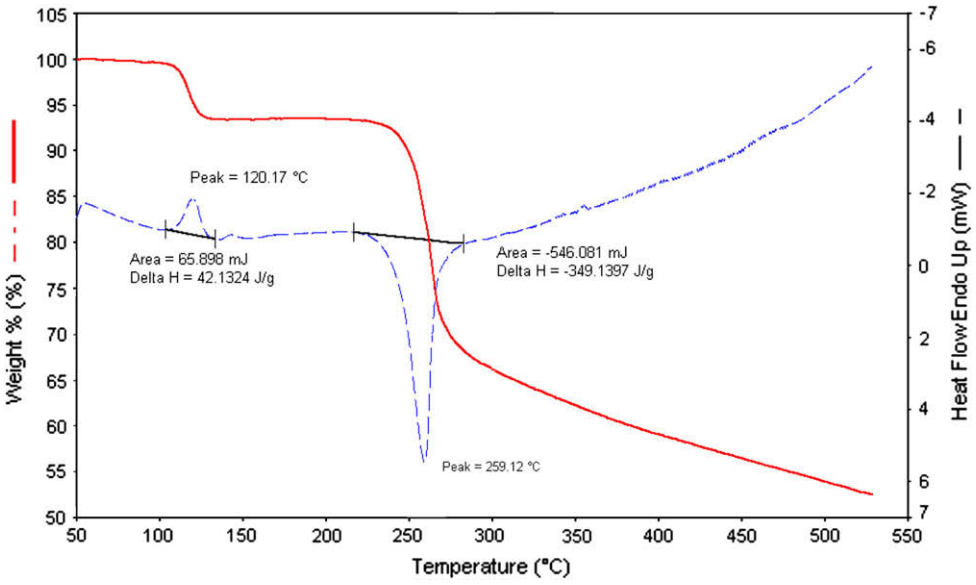

Fig. 5. TGA–DTA analyses curves of **3b**.

The TG curve for **1b**, refers to three stages of mass loses within the temperature range 50–550 °C. The first stage at 80–230 °C with a mass loss of 5.46% (calcd. 5.87%) corresponds to the loss of 1 mol ethanol molecule. The second stage at 240–290 °C with a mass loss of 22.70% (calcd. 22.80%) corresponds to the loss of C_6H_4 and NO_2 groups. The third stage of decomposition at the temperature range 300–550 °C is roughly assigned to the loss of remaining part of the organic ligand. The TG curve for **2b**, refers to two stages of mass loses within the temperature range 50–550 °C. The first stage at 245–285 °C with a mass loss of 26.10% (calcd. 26.58%) corresponds to the loss of $C_5H_6N_2O_2S_2$. The second stage of decomposition at the temperature range 300–550 °C, with a mass loss of 18.89% (calcd. 19.62%), corresponds to the loss of C_7H_5N. Also, **5b** shows similar degradation behavior and gives major decomposition in the temperature range of 235–275 °C and 280–550 °C, with weight loss of 25.75% and 20.40%, respectively. The first stage corresponds to the loss of $C_4H_4N_2O_2S_2$ (calcd. 25.10%) and the second stage of decomposition corresponds to the loss of C_8H_9N (calcd. 20.30%).

The DTA and TG curves showed that the **3b** exhibit an endothermic peak at about 120 °C and loss about 5.59% of its weight at 110–130 °C (Fig. 5), which corresponds to loss of one ethanol molecule (calcd. for C_2H_5OH, 5.53%). The second stage at 225–290 °C with a mass loss of 28.15% (calcd. 27.70%) corresponds to the loss of $C_5H_5N_4O_2S_2$. The third stage of decomposition at the temperature range 300–550 °C, with a mass loss of 21.20% (calcd. 21.03%), corresponds to the loss of $C_7H_7N_2$.

TG curve shows that the **4b** loses about 1.95%, 27.61% and 21.65% of its weight at 100–230, 240–290 and 300–550 °C, respectively. In the first stage, water molecule of lattice was released (calcd. 2.20%). The second and third stages indicate the loss of parts of the organic ligand, $C_5H_6N_4O_2S_2$ and $C_7H_7N_2$, respectively (calcd. 27.81% and 21.03%).

4. Conclusion

In the present work a series of new pyridazine-based azo chromophores were obtained by the condensation reaction of 3,6-bis((aminoethyl)thio)pyridazine with azo-coupled salicylaldehyde derivatives. The solvatochromic behaviors and substituent effects of the prepared compounds in various solvents were evaluated. The results indicated that the UV–vis spectra of these compounds were dependent on solvents polarity.

The all prepared compounds are stable up to 220 °C. The order of thermal stability found is **5b** > **3b** > **2b** > **1b** > **4b**. This fact should be related with the structure of the ligands and indicate the 4-nitro and 4-ethyl containing compounds are stable than others. According to the thermal stability of the prepared pyridazine-based azo compounds we can conclude that these compounds are suitable for use as recording dyes.

The TG/DTA and absorption spectra data of the prepared azo dyes (**1b**–**5b**) can be obtained free of charge via http://www.araku.ac.ir/~h_khanmohammadi/Supportinginformation-DYPI-D-08-0034.pdf.

Acknowledgments

We are grateful to the Arak University for financial support of this work.

Appendix. Supplementary material

Supplementary information associated with this article can be found in the online version, at doi:10.1016/j.dyepig.2008.07.019.

References

[1] Slater C, Rourke JP. Cyclometallated nitrogen heterocycles. J Org Chem 2003;688:112–20.
[2] Scheele UJ, Dechert S, Meyer F. A versatile access to pyridazines with tethered imidazolium groups: new precursors for mono- and binucleating NHC/pyridazine hybrid ligands. Tetrahedron Let 2007;48:8366–70.
[3] Abraham F, Langrenee M, Sueur S, Mernari B, Bremard C. Dicopper(II) complexes of novel polyfunctional pyridazines: crystal structure and magnetic properties of bis[(μ-pyridazine-3,6-dicarbaldehyde dioximato(1-)-N^1,N':N^2,N'')]-bis[aqua (perchlorato-*o*)copper(II)]. J Chem Soc Dalton Trans 1991:1443–7.
[4] Weitzer M, Brooker S. Dimetallic complexes of a structurally versatile pyridazine containing Schiff-base macrocyclic ligand with pendant pyridine arms. J Chem Soc Dalton Trans 2005:2448–54.
[5] Cuccia LA, Ruiz E, Lehn J-M, Homo J-C, Schmutz M. Helical self-organization and hierarchical self-assembly of an oligoheterocyclic pyridine-pyridazine strand into extended supramolecular fibers. Chem Eur J 2002;8:3448–57.
[6] Figueiredo H, Silva B, Raposo MMM, Fonseca AM, Neves I, Quintelas C, et al. Immobilization of Fe(III) complexes of pyridazine derivatives prepared from biosorbents supported on zeolites. Micropor Mesopor Mater 2008;109:163–71.
[7] Sönmez M, Berber İ, Akbas E. Synthesis, antibacterial and antifungal activity of some new pyridazinone metal complexes. Eur J Med Chem 2006;41:101–5.

[8] Gao H, Zhang Z-H, Jiang P, Li X-R. Synthesis, crystal structures and properties of the novel mononuclear copper(II) and tetranuclear cobalt(II) complexes with 3,6-bis-(3,5-dimethylpyrazolyl)-pyridazine. Transition Met Chem 2006;31:1088–92.
[9] Brooker S, Davidson TC, Hay SJ, Kelly RJ, Kennepohl DK, Plieger PG, et al. Doubly pyridazine-bridged macrocyclic complexes of copper in +1, +2 and mixed valent oxidation states. Coord Chem Rev 2001;216–217:3–30.
[10] Beckmann U, Brooker S. Cobalt(II) complexes of pyridazine or triazole containing ligands: spin-state control. Coord Chem Rev 2003;245:17–29.
[11] Sheppard CL, Tandon SS, Thompson LK, Bridson JN, Miller DO, Handa M, et al. Polynuclear copper(II) complexes with μ_2-1,1-azide bridges. Structural and magnetic properties. Inorg Chim Acta 1996;250:227–39.
[12] Thompson LK, Tandon SS, Manuel ME. Magneto-structural correlations in μ_2-1,1-azide-bridged dicopper(II) complexes. 2. Dominant antiferromagnetic coupling with azide bridge angles exceeding 108°. X-ray structures of [Cu_2(PAP) (μ_2-N_3)Br_3].cntdot.CH_2Cl_2, [Cu_2(PAP_6Me) (μ_2-N_3) (μ_2-Br)Br_2].1.68 H_2O, [Cu_2(PAP_6Me) (μ_2-N_3) (μ_2-H_2O) (NO_3)$_2$](NO_3).cntdot.0.75CH_3OH, [Cu_2 (PAN) (μ_2-N_3) (μ_2-NO_3) (NO_3)$_2$].CH_3OH·CH_3CN, and [Cu_2(PPh_3Me) (μ_2-N_3) Br_3(CH_3OH)]. Inorg Chem 1995;34:2356–66.
[13] Thompson LK, Mandal SK, Gabe EJ, Lee FL, Addison AW. Structure and electrochemical properties of antiferromagnetically coupled binuclear hydroxo-bridged copper(II) complexes with pyridazine and phthalazine ligands. Crystal and molecular structures of [μ-3,6-bis(1-pyrazolyl)pyridazine-N^2,μ-N^3,μ-N^4,N^5](μ-hydroxo)trichloroaquodicopper-(II)-0.8-water, $Cu_2C_{10}H_{11}C_{13}N_6O_2$·0.8$H_2O$ [μ-3,6-bis(1-pyrazolyl)pyridazine-N^2,μ-N^3,μ-N^4,N^5](μ-hydroxo)tribromoaquodicopper-(II)-0.6-water, $Cu_2C_{10}H_{11}Br_3N_6O_2$·0.6$H_2O$ and [μ-1,4-bis(1-methyl-2-imidazolyl)phthalazine](μ-hydroxo)tribromoaquodicopper(II)-water $Cu_2C_{16}H_{17}Br_3N_6O_3$·$H_2O$. Inorg Chem 1987;26:657–64.
[14] Kremer E, Facchin G, Estévez E, Alborés P, Baran EJ, Ellena J, et al. Copper complexes with heterocyclic sulfonamides: synthesis, spectroscopic characterization, microbiological and SOD-like activities: crystal structure of [Cu(sulfisoxazole)$_2$(H_2O)$_4$]·$2H_2O$. J Inorg Biochem 2006;100:1167–75.
[15] Bouffard J, Eaton RF, Müller P, Swager TM. Iptycene-derived pyridazines and phthalazines. J Org Chem 2007;72:10166–80.
[16] Bergthaller P, Stolzenburg R, Marx P. Photographical materials containing a pyridine azo or pyridazine azo cyan dye releasing compounds. US Patent 4,767,698; 1988.
[17] Deeb A, El-Mariah F, Hosny M. Pyridazine derivatives and related compounds. Part 13: synthesis and antimicrobial activity of some pyridazino[3′,4′:3,4]pyrazolo[5,1-c]-1,2,4-triazines. Bioorg Med Chem Lett 2004;14:5013–7.
[18] Brandt CD, Plieger PG, Kelly RJ, de Geest DJ, Kennepohl DK, Iremonger SS, et al. Dinickel(II), dizinc(II) and dilead(II) complexes of a pyridazine-containing Schiff-base macrocycle. Inorg Chim Acta 2004;357:4265–72.
[19] Brooker S, Plieger PG, Moubaraki B, Murrey KS. [Co^{II}_2L(NCS)$_2$(SCN)$_2$]: the first cobalt complex to exhibit both exchange coupling and spin crossover effects. Angew Chem Int Ed 1999;38:408–10.
[20] Brooker S, Ewing DD, Nelson J, Jeffery JC. Heterobinuclear cryptates; cooperative binding generates two different coordination sites within a symmetrical cryptand. Inorg Chim Acta 2002;337:463–6.
[21] Tandon SS, Thompson LK, Bridson JN. Dinuclear copper(II) and mixed-valence copper(II)–copper(I) complexes of 34-membered macrocyclic ligands (H_2M1, H_2M2) capable of forming endogenous phenolate and pyridazino bridges. X-ray crystal structures of the dinuclear copper(II) complexes [Cu_2M1][BF_4]$_2$·H_2O and [Cu_2M2][BF_4]$_2$·CH_3OH, which exhibit a remarkable ligand twist. Inorg Chem 1993;32:32.
[22] Tandon SS, Thompson LK, Bridson JN, Bubenik M. Synthesis and structural and magnetic properties of mononuclear, dinuclear, and tetranuclear copper(II) complexes of a 17-membered macrocyclic ligand (HM3), capable of forming endogenous phenoxide and pyridazino bridges. X-ray crystal structures of [Cu_2(M_3)$_2$(μ_2-OMe) (NO_3)$_2$], [Cu_4(M_3)$_2$(μ_3-OMe)$_2$(μ_2-Cl)$_2$$Cl_2$], [$Cu_4$($M_3$)$_2$($\mu_3$-OEt)$_2$($\mu_2$-$N_3$)$_2$($N_3$)$_2$](MeOH), [$Cu_4$($M_3$)$_2$($\mu_3$-OMe)$_2(NCS)_4$](DMF), and [Cu($M_3$) (NCS)$_2$]. Inorg Chem 1993;32:4621–31.
[23] Brooker S, Iremonger SS, Plieger PG. Bis(phenol-armed) pyridazine-containing Schiff base ligand: synthesis, complexation and reduction to the amine ligand analogue. Polyhedron 2003;22:665–71.
[24] Chen L, Thompson LK, Bridson JN. Coordination chemistry of thioether–pyridazine macrocycles. III. Synthetic, structural, and spectroscopic studies of Cu(II), Cu(II)Cu(I), and Cu(I) complexes of a hexathiapyridazinophane macrocyclic ligand. Can J Chem 1993;71:1086–93.
[25] Chen L, Thompson LK, Tandon SS, Bridson JN. Synthetic, structural, and spectroscopic studies on copper(II), copper(I), and silver(I) complexes of a series of pyridazinophane and phthalazinophane macrocycles, unusual extended metallocyclic structures. Inorg Chem 1993;32:4063–8.
[26] Robichaud P, Thompson LK. Binuclear copper(II) complexes of some potentially sexadentate phthalazine hydrazone ligands. Inorg Chim Acta 1984;85:137–42.
[27] Attanasio D, Dessy G, Fares V. Synthesis and properties of Mo(VI), Mo(V), Mo(IV) and mixed valence Mo(V)–Mo(IV) complexes with a binucleating Schiff's base. X-ray structure of the mononuclear *cis*-dioxo-aquo[1,4-dihydrazinophthalazine-bis(salicylideneiminato)] molybdenum(VI) acetone solvate. Inorg Chim Acta 1985;104:99–107.
[28] Nejati K, Rezvani Z, Massoumi B. Syntheses and investigation of thermal properties of copper complexes with azo-containing Schiff-base dyes. Dyes Pigments 2007;75:653–7.
[29] Zollinger H. Azo and diazochemistry. New York: Interscience; 1961.
[30] Nejati K, Rezvani Z. Syntheses, characterization and mesomorphic properties of new bis(alkoxyphenylazo)-substituted *N*,*N*′ salicylidene diiminato Ni(II), Cu(II) and VO(IV) complexes. New J Chem 2003;27:1665–9.
[31] Dinçaple H, Toker F, Durucasu İ, Avcibaşi N, Icli S. New thiophene-based azo ligands containing azo methine group in the main chain for the determination of copper(II) ions. Dyes Pigments 2007;75:11–24.
[32] Botros R. Azomethine dyes derived from an o-hydroxy aromatic aldehyde and a 2-aminopyridine. US Patent 4,051,119; 1977.
[33] Khedr AM, Gaber M, Issa RM, Erten H. Synthesis and spectral studies of 5-[3-1,2,4-triazolyl-azo]-2,4-dihydroxybenzaldehyde (TA) and its Schiff bases with 1,3-diaminopropane (TAAP) and 1,6-diaminohexane (TAAH). Their analytical application for spectrophotometric microdetermination of cobalt(II). Application in some radiochemical studies. Dyes Pigments 2005;67:117–26.
[34] Chen X, Zhang J, Zhang H, Jiang Z, Shi G, Li Y, et al. Preparation and nonlinear optical studies of a novel thermal stable polymer containing azo chromophores in the side chain. Dyes Pigments 2008;77:223–8.
[35] Qian Y, Wang G, Xiao G, Lin B, Cui Y. The first-order molecular hyperpolarizability and thermal stability of charge-transfer azo diol and azo aldimine. Dyes Pigments 2007;75:460–5.
[36] Mubarak MS, Peters DG. Survey of the electrochemical behavior of chlorinated pyrazines, quinoxalines, and pyridazines at carbon and mercury cathodes. J Electroanal Chem 2001;507:110–7.